

# 3 IMAGING TECHNIQUES

This chapter describes the methodologies used to reconstruct images. In this project images were reconstructed using real data acquired by the experimental system described in Chapter 2. Simulation work has also been conducted and the methodology will also be described in this chapter. Particularly, the model used to simulate the propagation of sound into the sand will be presented. The reconstruction techniques used are mostly based on the B-Mode technique that is described in Section 3.1. But many improvements of the conventional B-Mode algorithm are described in the following sections.

## 3.1 B-Mode Technique

The B-Mode algorithm is a simple but successful technique used in many ultrasound imaging systems. It is an easy processing technique, and in the case of ultrasound imaging it usually gives satisfying results. The B-Mode technique assumes a pulse-echo configuration, meaning that the same transducer is used on both transmit and receive. The pulse-echo systems are heavily utilized in diagnostic imaging—for example, echography [15] or cardiology [16].

### 3.1.1 Description

Assuming the pulse-echo configuration, a scan is moved along one direction. The transducer moves to one position, sends its pulse, records the echo signal, and then moves to next position. Most of the time the scan is linear; that is, the step size is constant and the path followed by the transducer is a straight line.

Then the echo signals are processed; they are filtered if necessary to keep only the frequency band of interest. The filtering also helps to reduce the noise. They are then envelope-detected using the Hilbert transform. The envelope-detected signals are converted into a decibel (dB) scale because the dynamic range of echo signals is often large and a logarithmic scale is hence necessary. Finally, the envelope-detected signals are displayed side by side

to form the image. Each echo signal is thus used to form a single column of the final image.

The way the scales of the picture are computed is simple. For the depth, also referred as range, it is a conversion from time to distance using the speed of propagation  $c$ ,  $d = ct$ . Because the signals are discrete we have to use  $d = cN/f_s$ , where  $N$  is the number of the sample and  $f_s$  the sampling frequency. The horizontal scale is determined by the step size of the scan. If the transducer moves 1 cm at each step, then each signal will be used to reconstruct a part of the final image 1 cm wide.

Figures 3.1 and 3.2 illustrate the different steps of the processing. In Figure 3.1, the top curve shows the raw echo signal where one can see the presence of high-frequency noise. The bottom plot shows in solid the low-pass-filtered raw data, and in dashed the envelope of the filtered signal. On Figure 3.2, the top plot is the envelope of the echo signal in a normalized decibel scale. Finally, the bottom picture of Figure 3.2 explains the way a single column of the final picture is built from this envelope in the decibel scale. Here, the raw signal was used to generate the column of the image between horizontal distances of 0.23 m and 0.24 m. This was done assuming a step size of 1 cm.

### 3.1.2 Pulse choice trade-off

The axial resolution is highly dependent upon the time-length of the pulse. Because when the pulse hits a target present in the medium and bounces back, the whole pulse is received. Hence, the length of the pulse is critical. For example, if one uses a sine wave composed of  $N$  cycles, when this pulse hits a target,  $N$  cycles are going to be received. Hence, a crude approximation of the axial resolution is  $N\lambda$ . Therefore, to increase the resolution it is interesting to send shorter pulses, that is, composed of less cycles at a higher frequency.

But when sending a pulse, even if it is composed of cycles of a perfect sine wave at a certain frequency, all the energy is not necessarily contained around that frequency. This is due to the effect of gating the pulse by a box window. Equation (3.1) describes a sine wave composed of  $N$  cycles at a frequency  $f_0$ .

$$s(t) = \sin(2\pi f_0 t) \text{rect}(f_0 t / N) \quad (3.1)$$

where  $\text{rect}(x)$  is defined by

$$rect(x) = \begin{cases} 1 & \text{for } |x| < 1/2 \\ 0 & \text{for } |x| \geq 1/2 \end{cases} \quad (3.2)$$

The Fourier transform of Equation (3.1) is

$$S(f) = \frac{\delta(f - f_0) - \delta(f + f_0)}{2j} \otimes \frac{N}{f_0} sinc(Nf/f_0) \quad (3.3)$$

where the sinc function is defined by  $sinc(t) = \frac{\sin(t)}{t}$ , and  $\otimes$  represents the convolution symbol.

Finally, using the properties of  $\delta$  functions we can easily obtain

$$S(f) = \frac{N}{2jf_0} sinc(N(f - f_0)/f_0) - sinc(N(f + f_0)/f_0) \quad (3.4)$$

The energy located around  $f_0$  can be approximated by

$$E(f) = \frac{N^2}{4f_0^2} sinc(N(f - f_0)/f_0)^2 \quad (3.5)$$

Integrating Equation (3.5) in the interval  $[f_0 - f_0\pi/N, f_0 + f_0\pi/N]$  will give us the energy located in the main lobe:

$$\int_{f_0 - f_0\pi/N}^{f_0 + f_0\pi/N} E(f) df = KN \int_{-\pi}^{\pi} sinc(t)^2 dt \quad (3.6)$$

$K$  is a constant independent on  $N$ , and the right-hand part of Equation (3.6) is obtained by a straightforward change of variable.

Finally since the last integral is converging and independent of  $N$ , Equation (3.6) shows that the energy located in the  $[f_0 - f_0\pi/N, f_0 + f_0\pi/N]$  frequency band is essentially proportional to  $N$ . Thus, the higher the value of  $N$ , the more energy is located around the frequency  $f_0$ .

When working with a transducer, it is important that the excitation pulse contain most of its energy around the resonance frequency of the transducer. This permits a better transmission of the energy into the medium. Therefore, the above demonstration shows that if we choose  $f_0$  to be the resonance frequency of the transducer, in order to maximize the transmission of energy we need to use more cycles.

This last fact show that there is a trade-off between transmitted energy and axial resolution. Fewer cycles lead to a shorter pulse and therefore a better axial resolution. And more cycles yield a better transmission of the energy into the medium.

### 3.1.3 Enhancements

The pictures constructed using the B-Mode technique described in Section 3.1.1 suffer from two main drawbacks.

The first is a direct consequence of attenuation. In the ideal case, if the medium encloses two similar targets we would like to see the same intensity for both targets on the final picture independently of the depths of the targets. This is of course not the case with the previous technique. If two targets are not located at the same depths, the wave does not have the same path to travel and will be attenuated differently. The technique used to compensate for attenuation due to the traveled distance in an attenuating material is called Time Gain Compensation (TGC).

TGC consists in compensating the received signals for the attenuation in the sand due to the distance traveled into the medium. To ensure that each time sample of each signal is multiplied by  $e^{\alpha ct}$ , where  $\alpha$  is the attenuation in Np/m,  $t$  the time in s and  $c$  the speed of propagation in m/s. Actually some compensation also has to be included for the spherical spreading of the wave. We can simply multiply each time sample of each signal by  $(c * t)^2$ . The square is present because we have to compensate in transmit and in receive of the same amount. And  $d = c * t$  is the distance traveled by the wave into the medium at that time. Therefore, the compensation needed is  $(c * t)^2$ .

The second drawback comes from the false assumption that the transmitter and receiver are located at the same position. It is of course false with our experimental system; our system is not a pulse-echo system but a pitch-catch system, where one transducer is used in transmit and another in receive. A consequence is that the conversion from time to depth is not linear. For example, if we denote by  $d_{T-R}$  the center-to-center distance between the transmitter and the receiver, and if we assume that the processing is done as if they were both located in the middle of the transmitter and receiver, then the error in the depth-scale introduced by the B-Mode technique would depend on the depth  $z_f$  following this simple relationship:

$$E_{z_f} = \frac{z_f - \sqrt{z_f^2 + \frac{d_{T-R}^2}{2}}}{c} \quad (3.7)$$

where  $c$  is the speed of propagation. This formula clearly shows that the error is most important at the air-sand interface, that is, when  $z_f = 0$ , and the error becomes 0 when  $z_f$  goes to infinity. But what Equation (3.7) shows

also is that this relationship is clearly nonlinear with respect to  $z_f$ . Also note that  $E_{z_f}$  has been defined so that it is always negative.

It is important to understand that because this imaging system is intended to do images at small depths, it is necessary to compensate this error. The technique is hence to pick a certain value of  $z_f$ , that is, the depth of focus. We then delay the received signals so that they arrive at  $z_f$  as if there was a transmitter-receiver element, the virtual element, located in the middle of the receiver-transmitter segment. The virtual element term means that we do processing so that we simulate a pulse-echo geometry and the virtual element is precisely the position for the transducer of the simulated pulse-echo geometry.

Throughout this thesis the expression “depth of focus” refers to a chosen depth used to do processing. This expression does not refer to the actual location of the focus of a transducer, as is often the case in ultrasonic literature.

If we denote by  $s(t)$  the received signal, to reconstruct a correct image with a depth of focus  $z_f$ , we will need to use  $s(t - 2E_{z_f})$ . The coefficient 2 is simply due to the fact that we have to compensate for two identical errors: first, the difference in travel time between the propagation from the source to the depth of focus and from the virtual source to the depth of focus, and second, for the difference in time travel between the propagation from the depth of focus to the receiver and the propagation between the depth of focus and the virtual receiver. This technique that corresponds to delaying the signals is often referred to as focusing. This technique corrects the error in the depth-time relationship. It therefore allows us to reconstruct a picture with a correct scale. But most of the picture is out of focus since the signals have delayed just to compensate the error for a single depth. An improvement of focusing, called dynamic focusing, allows for all the picture to be in focus. Dynamic focusing is mostly used with arrays and will be described in the next section.

## 3.2 Delay-and-Sum Beamforming

Delay-and-sum beamforming is an improvement of the B-Mode technique by using arrays. In our case we have a single transmitting element and a single receiving element; hence, we do not possess an array in the physical sense. But the flexibility of the system allows us to simulate any kind of array,– receiving array, transmitting array, or both– with any kind of geometry. Most of the work was conducted by simulating a receiving array. The

transmitting element was fixed at a certain position, and the receiver was moving and acquiring signals to simulate the array. Then the transmitter will move to its next position.

### 3.2.1 Description

The idea is simply to use all the signals from the receiving array to form one column of the final image. Because the signals are all acquired from different locations, they need to be delayed differently to focus at a certain depth  $z_f$ . Once all the signals are correctly delayed they are then averaged together and the same processing as in the B-Mode technique is used on this averaged signal to form one column from the final image.

Assuming a square receiving array of  $N_x \times N_y$  elements, the element-to-element distances are  $d_x$  and  $d_y$ . Also, the relative coordinates from the center of the array with respect to the transmitter are denoted by  $D_{TC_x}$  and  $D_{TC_y}$ .  $D_{TC} = \sqrt{D_{TC_x}^2 + D_{TC_y}^2}$  is therefore the distance between the transmitter and the center of the array. And  $z_f$  is the considered depth of focus. Finally, the virtual element is this time assumed to be in the middle of the transmitter and array center segment. It means that  $D_{TV}$ , the distance between the transmitter and the virtual element is,  $D_{TV} = \frac{D_{TC}}{2}$ . Figure 3.3 shows this geometry in the  $x - y$  plane (soil surface). The coordinate  $z$  is the depth into the soil.

We have then two kinds of delay:

- The delay  $t_T$  is the same for each receiver. It compensates for the difference in travel time from the actual source to the focal point and from the virtual source to the focal point. Figure 3.4 shows that this first delay is evaluated by

$$t_T = \frac{z_f}{c} - \frac{\sqrt{z_f^2 + D_{TV}^2}}{c} \quad (3.8)$$

- The delay  $t_{ij}$  is different for each receiving element. It compensates for the difference in travel times from the focal point to the actual receivers and from the focal point to the virtual receiver.

$$t_{ij} = \frac{z_f}{c} - \frac{\sqrt{z_f^2 + \left[\frac{D_{TC_x}}{2} + (i/2 - N_x)d_x\right]^2 + \left[\frac{D_{TC_y}}{2} + (j/2 - N_y)d_y\right]^2}}{c} \quad (3.9)$$

The terms  $[(i/2 - N_x)d_x]$  and  $[(j/2 - N_y)d_y]$  represents the  $(x, y)$  coordinates of the receiver  $(i, j)$  with respect to the center of the array. These values have to be added to the distance from the center of the array to the virtual element, terms  $\frac{D_T C_x}{2}$  and  $\frac{D_T C_y}{2}$  in Equation (3.9).

Then we compute  $g(t)$ , the average of the focused signals:

$$g(t) = \frac{1}{N_x N_y} \sum_{i,j} s_{i,j}(t - t_T - t_{ij}) \quad (3.10)$$

where  $s_{i,j}$  is the signal received by the receiver  $(i, j)$ . Finally, the image is built as in the B-Mode technique, by envelope detection and by displaying the  $g$ 's side by side.

### 3.2.2 Dynamic focusing

Dynamic focusing (DF) consists in focusing the signals, by delaying them, to many depths. Depths of focus are picked uniformly in the range of the image, then the signals are focused to all of the depths. To focus the signals to a certain depth, we delay each of them so that they arrive at the same time at the intended depth of focus. This is done using the method described in Section 3.2.1.

Then the image is reconstructed using the parts in focus of all these signals. For example, if we use five depths of focus on a 50-cm range, the signals are focused at the following depths: 5 cm, 15 cm, 25 cm, 35 cm, and 45 cm. Then only the signals focused at 5 cm are used to reconstruct the part of the image between the depths of 0 and 10 cm, only the signals focused at 15 cm are used to reconstruct the part of the image between the depths of 10 and 20 cm, and so on. This technique basically allows us to reconstruct images in focus at multiple discrete depths instead of at a single depth.

When the delayed signals are concatenated, discontinuities might appear because a signal focused at a certain depth has no reason of being continuous with the one focused at the next depth. To compensate for that, the signals were smoothed using weighted averages in the areas where they had to be connected.

## 3.3 Reconstruction Scripts

To reconstruct images using the B-Mode technique or the Delay-and-Sum Beamforming technique, scripts under the Matlab environment have been

developed. Moreover, for convenience and because of the similarity in processing for both techniques, the same scripts are able to handle both techniques.

Many versions have developed based on the ideas developed in Sections 3.1 and 3.2. The detailed Matlab sources can be found in Appendix A.

- `beamformer.m` : B-Mode technique and delay-and-sum with a single depth of focus.
- `beamformerTGC.m` : Time Gain Compensation is added to `beamformer.m`.
- `beamformerDFTGC.m` : Dynamic Focusing is added to `beamformerTGC.m`.
- `beamformerDFTGCsmooth.m` : Smoothing of the concatenated signals during the DF process is added to `beamformerDFTGC.m`.

### 3.4 Simulation of Received Signals

The propagation of acoustic waves into sand or any other porous and very attenuating medium can be modeled and simplified so that echo signals can be simulated. This section describes the methodology used to simulate the echo signals from the sand.

Having a means of simulating the system is very convenient because simulated data can be used to develop and validate new processing techniques.

#### 3.4.1 Model of acoustic propagation in sand

In the model, we consider the propagation of a wave at a speed  $c$  in an attenuating material whose attenuation constant is  $\alpha$  in Np/m.

Assume that the reflectivity function of the medium is  $\Gamma(x, y, z)$ . Ideally what we would like to retrieve from our model is  $|\Gamma|$  because it will mean a perfect reconstruction of the medium.

The pulse is  $s(t)$  and we consider the case of a single scatterer located at position  $(x, y, z)$  inside the medium. The transmitter is located at  $(x_t, y_t, 0)$  and the receiver at  $(x_r, y_r, 0)$ ; the  $z$ -coordinates are 0 because the transducers are in contact with the soil (the  $x-y$  plane). Then the echo signal generated by this scatterer is

$$\tilde{s}_{x,y,z}(t) = \Gamma(x, y, z) \frac{s(t - D/c) e^{-\alpha(D_1 + D_2)}}{D_1 D_2} \quad (3.11)$$



where  $D$  is the total distance traveled by the wave,  $D_1$  is the distance from the source to the point scatterer, and  $D_2$  the distance from the point scatterer to the receiver. These values are computed by

$$D_1 = \sqrt{(x - x_t)^2 + (y - y_t)^2 + z^2} \quad (3.12)$$

$$D_2 = \sqrt{(x - x_r)^2 + (y - y_r)^2 + z^2} \quad (3.13)$$

$$D = D_1 + D_2 \quad (3.14)$$

The term  $s(t - D/c)$  in Equation (3.11) represents a delayed version of the pulse due to the time necessary to travel from the source to the point scatterer and then to the receiver. The exponential term represents the attenuation due to the medium. And the term in the denominator is here to express the spherical spreadings of the transmitter ( $D_1$ ) and of the receiver ( $D_2$ ). Finally a multiplication by  $\Gamma(x, y, z)$  is necessary because it is the value of the reflectivity of the considered scatterer.

In this model, it is important to understand the limit of Equation (3.11) in terms of attenuation due to the propagation. The exponential term assumes an attenuation constant in frequency. This assumption is false as it has been shown that the attenuation increases with frequency and is not far from being linear with frequency [11]. The pulse  $s(t)$  does not have a single frequency component. So the attenuation is only an approximation of the real attenuation due to the medium. A more correct model would consist in attenuating in the frequency domain, attenuating each frequency component with the right exponential term. But such a model would make the simulations take a much longer time.

This model also assumes that the receiver and transmitter are a point-receiver and point-transmitter. This assumption is incorrect. But at the usual frequency of operation, 2 kHz, the transducers are very omnidirectional. Their behaviors are therefore very close to point source. However, to be more accurate we could simply integrate Equation (3.11) over the surfaces of both transducers.

Finally, to get the actual received signals we need to account for all the scatterers in the medium. We integrate Equation (3.11) over all the media:

$$\tilde{s}(t) = \int_{x_{min}}^{x_{max}} \int_{y_{min}}^{y_{max}} \int_0^{z_{max}} \tilde{s}_{x,y,z}(t) dx dy dz \quad (3.15)$$

### 3.4.2 Computer program

Based on Equation (3.15) a computer program has been developed. This program used to simulate the received signals from the sandbox is an adaptation of the previous work of Frazier et al. on the actual system [14].

The transmitted pulse is a sine wave whose center frequency and number of cycles are variables.

The program simply computes the integral described in Equation (3.15). Of course, the computer cannot handle continuous sums; hence, the program uses a 3D grid and considers each point of this grid as a scatterer with a certain reflection coefficient. The echo signals of all points are summed to account for all scatterers in the medium, and then summed again over the circular surface of the receiving element.

The transmitter is assumed to be a point-element transmitter. However, the receiver can be either a point receiver or a circular receiver. When the receiver is a circular receiver the surface is also discrete and signals are then summed over the surface.

All the parameters necessary to describe the geometry of the scan as well as the acoustical properties of the medium are entered into an external text file. This file will be referred later as the parameter file. The scan is always assumed to be linear in the  $y$  direction, which is not a limitation because we can simulate any kind of array in receive at any locations.

Another text file is used to describe the target present in the medium and will be referred as the point scatterer file.

The program of Nail Cadalli, as well as its new version was developed in C++ in the Unix environment. The repeated computation of Equation (3.15) would be straightforward in the MATLAB environment. But a MATLAB program would not be able to run in a satisfying time because an average simulation already takes around 20 hours with an optimized C++ code on a fast Sun workstation. The source of this program, called SimSignal, can be found in Appendix B.

### 3.4.3 Parameter file

This file describes the geometry of the scan, the sampling grid as well as the acoustical properties of the medium. Following is a sample of this file:

Speed of propagation in m/s

PSS=200

Center frequency of the pulse in Hz

freq=2000

Number of cycles  
CycleCount=2

Attenuation in Np/m  
alpha=13.8

Diameter of the source in meter  
DiamTrans=0.078

Diameter of the receiver in meter  
DiamRec=0.051

Initial position of the transmitter in meter  
xxt=0.0  
yyt=0.0

Number of array elements in the X direction  
Ndx=1

Number of array elements in the Y direction  
Ndy=10

Number of points of the grid in the X direction  
Nx=50

Number of points of the grid in the Y direction  
Ny=50

Number of points of the grid in the Z direction  
Nz=60

Number of time sample in the received signals  
Nt=1 024

Number of sample over the receiver surface  
Np=4

Number of depths of focus for dynamic focusing  
Ndeep=5

Number of realization of the random scattering noise  
Nr=1

Number of steps of the scan  
Na=30

Step size of the scan in cm  
da=0.01

Starting point of the center of the array  
ya1=-0.15

Sides of the sampled space  
xx1=-0.5  
xx2=0.5  
yy1=-0.5

yy2=0.5

zz1=0

zz2=0.5

Beginning of the time of interest in the received signals in seconds

tt1=0

For later use, will be used to describe complex targets

ox1=0

ox2=0.1

oy1=0

oy2=0.1

oz1=0.1

oz2=0.7

Offset of the array in meters

SensorPositionx0=0.0

SensorPositiony0=0.0

Inter element spacing in meters

SensorSpacingx=0.01

SensorSpacingy=0.01

Maximum value of the scattering noise

MaxNoise=0.000 000 5

Sampling frequency in Hz

SamplingFreq=60 060

Use of object (keep to 1)

object\_exists=1

Two for use of the scattering points file, otherwise use hardcoded objects

object\_mode=2

If not 0 write log files

wrt\_file=0

If 0, no noise.

noisy=0

### 3.4.4 Points scatterers file

This file describes what is present in the medium and looks like

(0.0,0.0,0.2)=1.0

(0.0,0.1,0.2)=1.0

This simply says that there are targets with reflection coefficient of unity (1.0) at the locations (0,0,0.2) and (0,0.1,0.2) in meters. As many points as wanted can be included in this file.

### 3.4.5 Use of the program

The simulator executable program is called SimSignal. Its use is very simple.

Type:

SimSignal < *T* >< *Rec* >< *Param* >< *Points* >

where T is the file where the transmitted pulse is saved. Rec is the core of the received signals (Rec\_0, Rec\_1 and so on are then the received signals files). Param is the parameter file name, and Points is the point scatterers file.

This program saves one file for each receiving position for each step of the scan. This is because the experimental system saves the echo signals the same way. The fact that the files are saved in the same format is convenient for testing the same reconstruction algorithm on both simulated and experimental data. The reconstruction scripts described in Section 3.3 are able to reconstruct images from experimental data as well as simulated data.

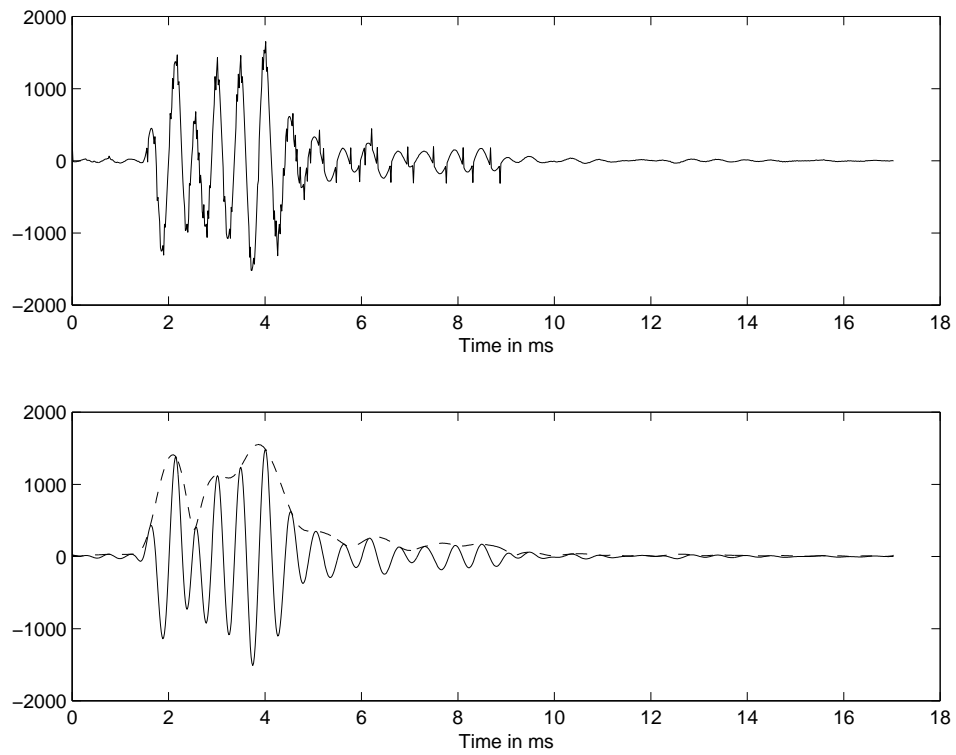


Figure 3.1: Description of the B-Mode imaging technique. Top: Raw echo signal. Bottom: Low-pass-filtered raw echo signal (solid) and envelope detected by Hilbert transform (dashed).

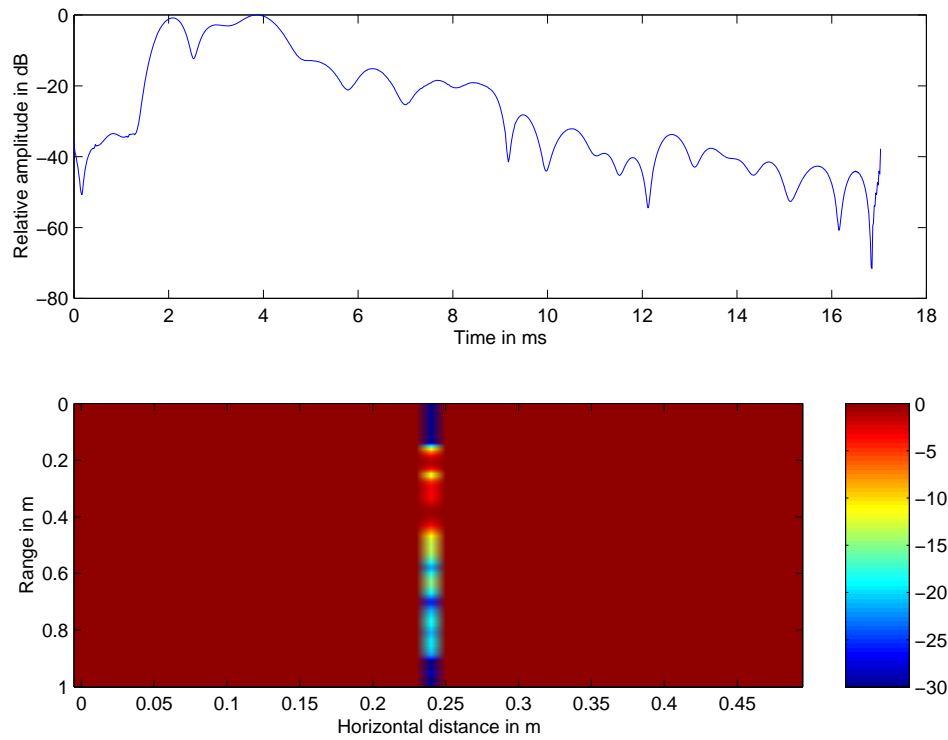


Figure 3.2: Description of the B-Mode imaging technique. Top: Envelope of filtered echo signal in dB. Bottom: Display of the dB scale envelope to form one single column of the picture.

- Fixed transmitter position
- Receiving positions
- Receiving array center
- Virtual element

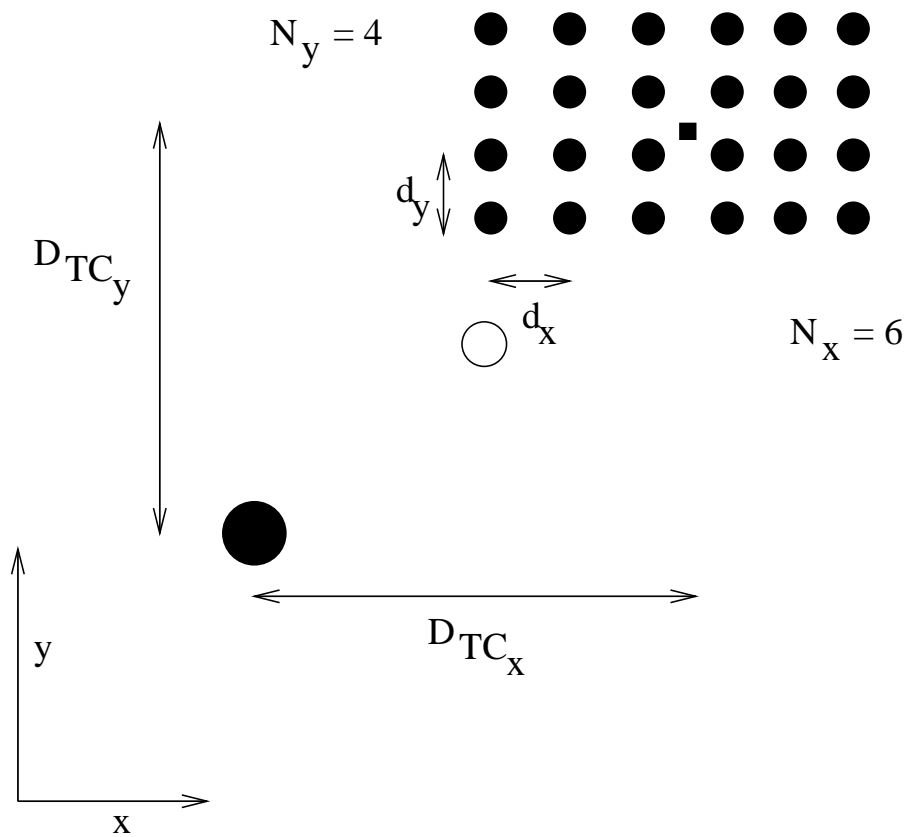


Figure 3.3: Geometry used to compute delays when a receiving array is simulated. The figure is in the  $x$ - $y$  plane which is the sand surface.



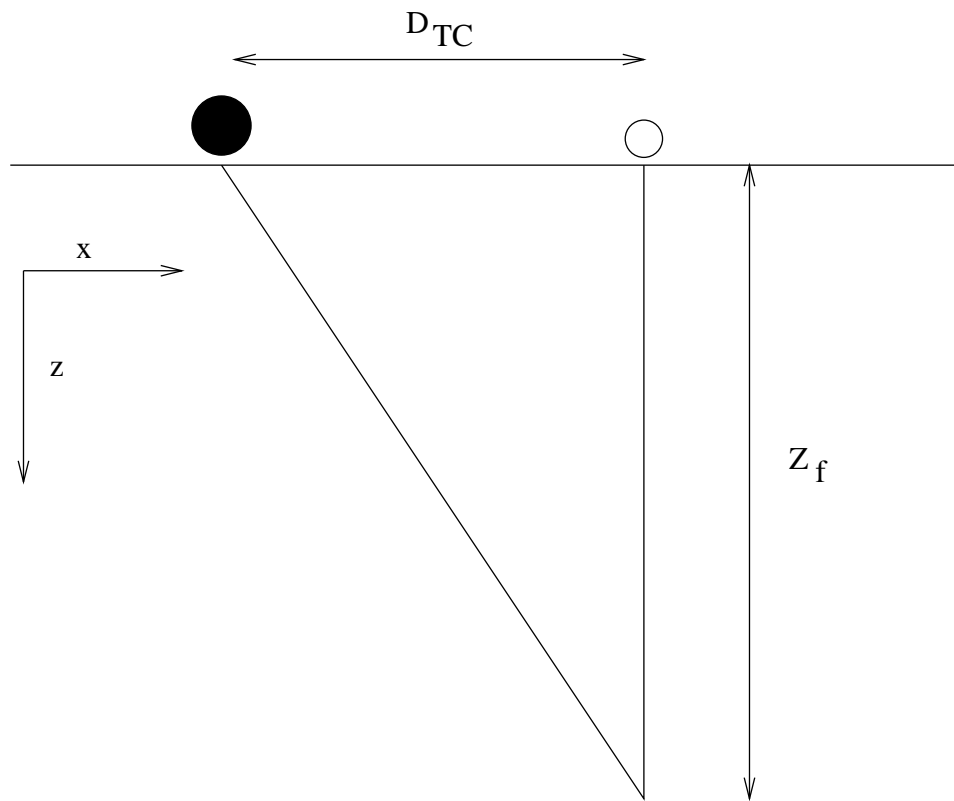


Figure 3.4: Geometry used to compute delays when a receiving array is simulated. The figure is in the  $x$ - $z$  plane.